

IONIC TRANSPORT IN TALL COLUMNAR EPITHELIAL (TCE) CELLS OBTAINED BY NASAL BRUSHING FROM NON-CYSTIC FIBROSIS (CF) INDIVIDUALS

ANA C. MAURÍCIO, D. PENQUE, M. D. AMARAL, K. T. G. FERREIRA*

Departamento de Clínicas Veterinárias, Instituto de Ciências Biomédicas de Abel Salazar. Universidade do Porto. Centro de Genética Humana. Instituto Nacional de Saúde Dr. Ricardo Jorge. Departamento de Química e Bioquímica. Faculdade de Ciências. Universidade de Lisboa. Centro de Química Fina e Biotecnologia. Faculdade de Ciências e Tecnologia. Universidade Nova de Lisboa.

SUMMARY

Tall columnar epithelial (TCE) cells can be obtained by a non-invasive procedure through brushing the inferior turbinate and the adjacent lateral nasal wall. Here, we present results from the functional study of epithelial cells, thus obtained by using the patch-clamp technique. By patch-clamping the sub-apical region of TCE cells, we were able to identify at least three different groups of Cl⁻ channels, namely: a) one with large conductance, rectifying, which was the most frequently found type of Cl⁻ channel; b) a second type of small conductance, activated by cAMP and IBMX, in excised inside-out patches and voltage independent; c) a third type with a conductance around 25 pS, voltage independent, with a linear IV relationship, that could be observed in the excised inside-out configuration. The study of CFTR Cl⁻ channel and its role in airway cell physiology has generally been conducted in cultured cells, most of which not polarized. This experimental work using freshly obtained TCE cells from the nasal epithelium, demonstrates that such cells may be one valid tool to study Cl⁻ channels (most probably ORCC and CFTR Cl⁻ channels) as a model for the lower respiratory epithelium.

Keywords: tall columnar epithelial (TCE) cells, CFTR, nasal brushing, patch-clamp, chloride, ORCC, functional assessment.

RESUMO

TRANSPORTE IÓNICO DE CÉLULAS EPITELIAIS COLUNARES ALTAS (TCE) OBTIDAS POR RASPAGEM NASAL EM INDIVÍDUOS SEM FIBROSE QUÍSTICA (FQ).

As células epiteliais colunares altas (TCE) podem ser obtidas por um método não invasivo, através da raspagem da mucosa que reveste o turbinado inferior e a parede nasal lateral adjacente. Neste trabalho, serão apresentados resultados obtidos com um estudo funcional destas células epiteliais através da aplicação da técnica de retalho controlado (ou *patch clamp*). A micropipeta é encostada à região sub-apical das células TCE de forma a obter um giga-selo, permitindo a observação com elevada resolução de correntes provenientes de um canal iónico. Com esta técnica, conseguimos identificar três grupos diferentes de canais de Cl⁻, nomeadamente: a) um grupo de canais com uma

*A convite da AMP

grande conductância, que rectificam, que foram os mais frequentes; b) um segundo tipo de canais de Cl⁻, de pequena conductância, activados pelo cAMP e pelo IBMX, em retalhos de membrana celular na configuração *excised inside-out* e independentes da voltagem; c) um terceiro grupo, com uma conductância média de 25 pS, independentes da voltagem, com uma relação IV linear e que foram igualmente observados em retalhos de membrana celular na configuração *excised inside-out*. O estudo do canal de Cl⁻ CFTR e o seu papel na fisiologia celular das vias respiratórias, tem sido conduzido em culturas celulares, grande parte das vezes, não polarizadas. Este trabalho experimental, utilizando células TCE frescas, obtidas do epitélio nasal de indivíduos, demonstra que estas células podem ser um instrumento válido para estudar o transporte iónico de Cl⁻ (principalmente canais de Cl⁻ do tipo CFTR e ORCC), funcionando como um importante modelo do epitélio do tracto respiratório inferior humano.

Palavras-chave: células epiteliais colunares altas (ECT), CFTR, raspagem nasal, retalho-controlado, cloro, ORCC, estudo funcional.

INTRODUCTION

Cystic Fibrosis (CF) is a common inherited disease that is characterized by a defective cAMP-regulated chloride (Cl⁻) conductance due to impaired function of the CF Transmembrane Conductance Regulator (CFTR) protein. CFTR is a member of the ATP-binding cassette (ABC) transporter family that forms a Cl⁻ channel with complex regulation. It functions not only as a Cl⁻ and bicarbonate channel^{1,2} but also as a regulator of sodium (Na⁺) channels³ and of outwardly rectifying chloride channels^{4,5} (ORCC). Results from a number of groups are consistent with the concept of at least two pathways of CFTR activation by cAMP, namely: 1) membrane inserted CFTR Cl⁻ channels are activated directly by cAMP, and 2) traffic activation of CFTR from intracellular pool to the plasma membrane, occurring via cAMP- and Ca²⁺-dependent PKA-mediated exocytosis, as first suggested by Bradbury *et al.* in 1992⁶ and also by other authors⁷⁻¹¹. ORCC has been the subject of considerable electrophysiological interest over the past 10 years, and is well characterized at the single channel level¹², but its physiological function in epithelial cells, including those from the respiratory tract, remains controversial¹³. Measurements of the nasal potential difference (NPD) consistently demonstrated increased values in CF patients¹⁴⁻¹⁷. Additionally, some CF patients, regardless of genotype, have a limited ability to secrete Cl⁻ when stimulated by Cl⁻ secretagogues, and this residual secretion, assessed as NPD, has been shown to correlate with a better lung function¹⁸. The nasal epithelium thus reflects the general dysfunction occurring in the lower airways of CF patients. Many studies on CFTR and on its role in airway cell physiology are conducted in cultured cells,

most of which not polarized. However, culture conditions, proliferation, and possibly also immortalization, influence the differentiation state, which in turn affects CFTR expression levels, traffic and processing^{19,13,20}. We have previously used freshly obtained cells from the nasal epithelium to analyse CFTR transcripts^{21,22}, and also to determine the intracellular localization of normal and F508del-CFTR, the most frequent mutant in CF^{23,24}. We have previously shown, by immunocytochemical techniques²³ that the proportion of tall columnar epithelial (TCE) cells (ciliated and non-ciliated) with CFTR protein in the apical region is significantly higher in normal individuals (about 60%) than in CF patients homozygous for F508del (about 20%). The fact that some F508del-CFTR protein reaches the apical region (including both apical and sub-apical) in native tissues is in contrast with the complete endoplasmic reticulum (ER) retention described in heterologous expression systems, *i.e.*, transfected cell lines. Here, we tested whether these freshly obtained nasal TCE cells, which have not been treated with enzymes, can also be used to assess CFTR as Cl⁻ channel function in the airways, and possibly be used as a diagnostic tool to distinguish between individuals with and without CF. We thus examined the Cl⁻ conductance in the sub-apical region (to avoid the ciliated area) of fresh TCE cells, obtained by the nasal brushing technique from non-CF individuals, by patch-clamp in the cell-attached and excised inside-out configurations.

METHODS

Isolation of TCE cells from non-CF patients

Following informed consent, cells from nasal brushings

were obtained from non-CF individuals (N = 8) with neither clinical signs of CF nor the F508del mutation, as determined by genomic DNA analysis, performed as described before²⁵. Cells from the nasal epithelium (see figure 1A) were obtained also as previously described²¹. Briefly, we used an interdental brush with 2.5 – 3 mm bristles (Paro-Isola, Thalwil, Switzerland) to scrape along the tip of the inferior turbinate and the adjacent lateral nasal wall. Brushes containing cells were immediately placed into an end-cut automatic pipette tip (P200) inside a plastic tube with phosphate buffer saline (PBS) pH 7.4 at room temperature. Cells were removed from the brush by flicking it up and down inside the tip. Cells were collected by centrifugation at 3.000 rpm in a picofuge™ (Stratagene, La Jolla, CA) for 4 min. This procedure, thus completely avoided the use of proteolytic enzymes to obtain isolated cells. For cytological examination and immunocytochemistry, cells were gently re-suspended from the pellet in fixing solution and analyzed as previously described²³. Cells used for patch-clamp experiments, had a slightly different treatment. They were re-suspended and washed three times in solution B2 (see table I) with the following composition (mM): NaCl 127, KCl 5, Na-pyruvate 5, D-glucose 5, 4-(2-hydroxyethyl)-1-piperazinethanesulphonic acid (HEPES) 10, CaCl₂ 1.25 and MgCl₂ 1. Albumin 10% (w/v) was added to solution B2. The suspension was centrifuged (and the pellet re-suspended) 3 times at 30 g for 1 min, at room temperature. Solution B2 (see table I) containing 3 mM dithiothreitol, DTT (Sigma), and 1 mg/ml hyaluronidase (Sigma) as mucolytic agents, was added to the final washed pellet and maintained at 4°C until the beginning of the experiment. 20 µl of this cell suspension were diluted in the bath solution (solution P1) and transferred into a Petri dish previously coated with poly-L-lysine and mounted on the stage of an inverted microscope (Axiovert 25, Zeiss, Germany). The patch-clamp experiments were performed directly on the sub-apical region of the TCE cells (see figure 1C). A permanent flux of bath solution was maintained during the recordings, with a rapid solution changer associated to a vacuum pump.

Cytological evaluation of tall columnar epithelial (TCE) cells recovered by nasal brushing

The freshly isolated human cells recovered from nasal brushings and spread on silane glass slides were stained by the May-Grünwald-Giemsa (MGG) method²⁶. Samples on slides were evaluated for cell differential count and morphology on a conventional light microscope (Zeiss, Jena, Germany) at 100X magnification under oil immersion. TCE cells were identified on the basis of criteria described by other authors²⁷, namely, those with columnar shapes

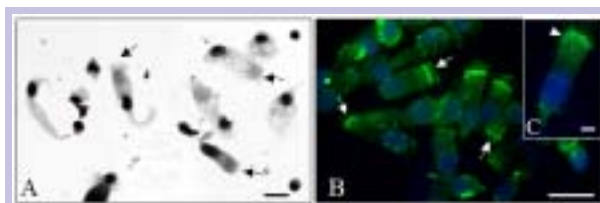


Fig. 1 - (A) Analysis of nasal cells recovered by brushing by MGG-staining (see “Material and Methods”). The major type of cells is tall columnar epithelial (TCE) cells, ciliated or not, amounting, on average, to approximately 65% of all cells recovered by the brushing procedure. The apical site of TCE cells is indicated by arrows. Bar: 50 µm. (B) Nasal-brushing cells immuno-stained with monoclonal Ab to detect CFTR protein (see “Material and Methods”). CFTR staining is clearly detected as a green line at the apical region of TCE cells (see arrowheads). Bar: 50 µm. (C) Magnification of one cell as in B, evidencing the sub-apical region (see arrowhead) where the pipette was attached for the patch-clamp experiments. Bar: 20 µm.

| | P1 | B1 | B2 |
|------------------|-----|-------|-------|
| Na ⁺ | 140 | 5 | 132 |
| K ⁺ | 5 | 140 | 5 |
| Ca ²⁺ | 1 | 0.1 | 1.25 |
| Mg ²⁺ | 1 | 1 | 1 |
| Cl ⁻ | 149 | 147.2 | 136.5 |
| D-glucose | - | - | 5 |
| Pyruvate | - | - | 5 |
| HEPES | 10 | 10 | 10 |
| EGTA | - | 1 | - |
| ATP | - | 1 | - |
| pH | 7.4 | 7.2 | 7.4 |

Table I - Composition (mM) of the solutions used in the patch-clamp experiments.

P, pipette solution; B, bath solution. HEPES, 4-(2-hydroxyethyl)-1-piperazinethanesulphonic acid; EGTA, ethylene glycol-bis(β-aminoethyl ether)-N,N,N',N'-tetraacetate; ATP, adenosine-3,5-triphosphate.

with or without cilia. Since secretory goblet cells have similar shape but no cilia, they were also included in the group of TCE cells. All other cells that did not meet this criterion such as basal cells and inflammatory cells (see figure 1A) were excluded from this group.

Immunocytochemistry

The intracellular localization of CFTR in nasal brushing cells was analyzed by immunocytochemistry as described before²³ using the monoclonal antibody (Ab) M13-1 (Genzyme, Cambridge, MA), raised against amino acids 729-736 of the R-domain²⁸ (Gregory *et al.*, 1990). Briefly, after fixation on slides (see above), cells were rinsed for 5 min with cold PBS and incubated with methanol for 5 min at -20°C, followed by two washes with PBS and incuba-

tion with 0.25% (v/v) Triton X-100 in PBS for 10 min, for cell permeabilization. Nonspecific staining was blocked by incubating cells with 1% (w/v) BSA in PBS for 30 min. Slides were then incubated with the M13-1 Ab diluted 1:20 in 0.5% (w/v) bovine serum albumin (BSA) in PBS overnight at 4°C. Cells were then washed three times 5 min with PBS, incubated with the secondary Ab, *i.e.*, FITC-conjugated anti-mouse IgG (Boehringer Mannheim, Germany) diluted 1:80 in 0.5% (w/v) BSA in PBS for 30 min, and washed as described above. Slides were mounted with Vectashield (Vector Laboratories, Inc., Burlingame, CA) containing DAPI (4,6-diamino-2-phenylindole, from Sigma Chemical Co) as a nuclear stain and covered with a glass cover slip. Immunofluorescence staining was observed and collected on an Axioskop fluorescence microscope (Zeiss, Jena, Germany) with the Power Gene 810/Probe &CGH software system (PSI, Chester, UK).

Patch-clamp experiments

Cell-attached and excised inside-out patch-clamp configurations were used for studies of single-channel activity. All the glass capillary tubes for the pipette fabrication were purchased from Science Products GmbH (Hofheim, Germany). The type of pipette used was thick-walled glass, filamented and with a 150 μm outer diameter (GB150F-8P). All the pipettes were pulled using the two stage pulling procedure described by Hamil *et al.*, in 1981²⁹ in a vertical micropipette puller (Narishige, Tokyo, Japan) and the tips fire polished using a microforge (our own fabrication). All the filling solutions were filtered using a sterile 0.22 μm -syringe filter (Millipore, Bedford, MA). The pipettes had resistances ranging from 10 to 12 MW. For the cell-attached experiments, the applied voltage ranged from -120 to +140 mV. The voltage protocol consisted of 14 steps of 20 mV (figure 2). For the excised inside-out configuration, the applied voltage ranged from -140 to +120 mV (figure 3), -160 to +100 mV (figure 4) or -120 to +140 mV (figures 5, 6 and 7), in steps of 20 mV. The membrane potential from cell-attached patches (V_{memb}) was determined using the cell potential (V_{cell}) as well as the applied pipette potential (V_{pip}). The membrane potential was therefore calculated as $V_{\text{memb}} = V_{\text{cell}} - V_{\text{pip}}$, considering $V_{\text{cell}} = -30 \pm 1.7$ mV ($N = 29$). The membrane potential was determined in 29 TCE cells by measuring the potential for $I = 0$, immediately after the performance of the whole-cell configuration. These experiments were performed at room temperature (22 – 23°C) with Axopatch 200A integrating patch-clamp amplifier (Axon Instruments Inc, Union City, CA, USA).

The data analysis was done with Clampfit 6 software (Axon). The single-channel experiments were filtered at 1 kHz. The reference electrode used in our experiments was

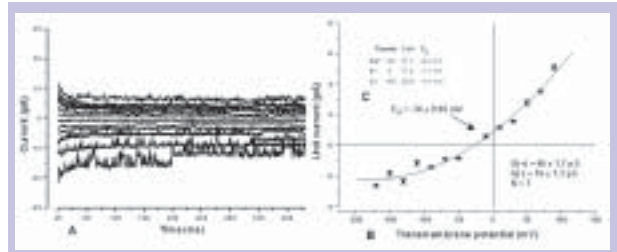


Fig. 2A - Shows an original trace of current (in pA) versus time (in ms), obtained in the cell-attached configuration. The voltage protocol consisted in 14 steps of 20 mV, ranging from -120 mV to +140 mV. The original trace is inverted. Solution P1 (see table I) was used in the pipette and in the bath.

Fig. 2B - Represents the IV curve where mean unit currents (in pA) were plotted against applied voltage (in mV), resulting from the analysis of 7 patch clamp experiments with TCE cells ($N = 7$). The IV curve was corrected for an intracellular potential of -30 mV. The conductance (G) and reversal potential (E_{r}) were obtained by linear regression. The conductance values for the positive and negative part of the curve were 46 ± 1.7 pS and 16 ± 1.3 pS, respectively. The reversal potential was -34 ± 0.96 mV. **Inset 2C** - Shows the concentration of Na^+ , K^+ and Cl^- in the pipette solution and in the cytosol and the respective calculated reversal potentials (E_{r}) for these experimental conditions.

a silver wire coated with silver chloride, embedded in an agar bridge made up with 1 M KCl. Positive currents correspond to the flow of positive charges across the membrane from the inside of the cell towards the outside or to the flow of negative charges in the opposite direction. The applied electrical potential (in mV) is defined as the difference between the compartment bathing the inside of the membrane and the compartment bathing the outside (reference electrode).

Composition of bathing and pipette solutions

The composition of the solutions used is shown in table I. The osmolality of the solutions used in the experiments with TCE cells was 290 mOsmol kg^{-1} . Drugs used in this study included: cAMP (0.1 mM) and isobutylmethylxanthine (IBMX, 0.1 mM). All chemicals used were of the highest grade of purity available and were obtained from either Sigma or Merck (Darmstadt, Germany).

Statistical analysis

Results are presented as mean and standard error of the mean (SEM). N corresponds to the number of TCE cells analyzed. All statistical tests were Student's t test³⁰. The P values given correspond to errors of the second kind.

RESULTS

TCE cells present CFTR in the apical region and are the major cell type recovered by nasal brushing

Nasal brushing samples from non-CF individuals ($N =$

8) were MGG-stained as described^{23, 24} to evaluate the cellular types recovered. As shown in figure 1A, TCE cells (ciliated or not) were the predominant class, accounting for approximately 65% of all cells. The presence of CFTR in the apical membrane of TCE cell was confirmed by immunostaining with an anti-CFTR Ab, as described in the Materials and Methods section (figure 1B). As we have previously described²¹, CFTR-staining is mostly observed in a broad area at the apical region of TCE cells, *i.e.*, consistent with both apical and sub-apical localizations. Taking these results into account, the patch-clamp analysis of these cells was performed on the sub-apical region of the cells, thus avoiding the ciliated area (see arrow head in inset 1C).

Studies of TCE cells by the patch-clamp technique in the cell-attached configuration

Figure 2 (panel A) shows an original trace of current (in pA) versus time (in ms), at different steps of the voltage protocol obtained in the cell-attached configuration of a TCE cell. In these experiments the same solution (solution P1, table I) was used both in the pipette and in the bath. The cell-attached patches presented spontaneous single-channel activity in the negative and positive voltage steps. Panel 2B represents a current-voltage (IV) curve where mean unit currents (in pA) were plotted against the transmembrane potential (in mV). This is the result of the analysis of original traces obtained with 7 TCE cells ($N = 7$), in the cell-attached configuration. The resulting IV curve was corrected for an intracellular potential of -30 mV. Inset 2C shows the concentration of Na^+ , K^+ and Cl^- in the pipette solution and in the cytosol³¹, and the respective calculated reversal potentials (E_R) for these experimental conditions. The conductances and reversal potentials were obtained by linear regression. The IV curve presented outward rectification. The conductance values for the positive and negative part of the curve were 46 ± 1.7 pS and 16 ± 1.3 pS, respectively. The reversal potential was -34 ± 0.96 mV. The value calculated for Cl^- under these experimental conditions was -41 mV (solution P1: 149 mM; cytosol: 29.6 mM; $E_{\text{Cl}} = -41$ mV). The reversal potential was statistically different from the one expected for Cl^- for an error of the second kind < 0.05 ($t = 7.64$; $p = 2.618 \times 10^{-4}$; $f = 6$).

Studies of TCE cells by the patch-clamp technique in the excised inside-out configuration

Figure 3A shows an original trace of current (in pA) versus time (in ms) at different steps of voltage protocol obtained in the excised inside-out configuration. In all excised inside-out experiments, solutions B1 and P1 (see table I) were used in the bath and pipette, respectively. These excised inside-out patches presented spontaneous

single channel activity in the negative and positive voltage steps. Excised inside-out unit currents from patch experiments with 6 TCE cells were measured ($N = 6$). The resulting IV curve is plotted in figure 3B and presented an outward rectification. Inset 3C shows the concentration of Na^+ , K^+ and Cl^- in the pipette and in the bath solutions and the respective calculated reversal potentials for these experimental conditions. The single-channel conductance, calculated by linear regression was 35 ± 1.4 pS for the positive and 17 ± 1 pS for the negative applied voltages. The reversal potential of -0.73 ± 0.8 mV was not statistically different from the one expected for Cl^- in these experimental conditions (0 mV) for an error of the second kind < 0.05 ($t = -0.96$; $p = 0.3804$; $f = 5$).

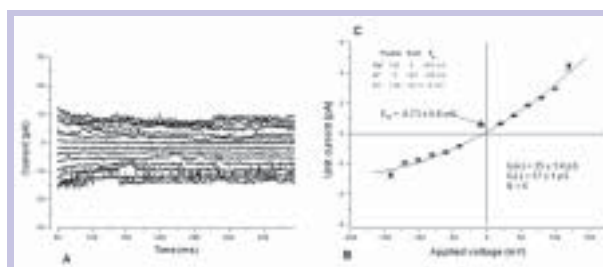


Fig. 3A - Shows an original trace of current (in pA) versus time (in ms) at different steps of the voltage protocol obtained in the excised inside-out configuration. The voltage protocol consisted in 14 steps of 20 mV ranging from -140 mV to +120 mV. Solutions B1 and P1 (see table I) were used in the bath and in the pipette, respectively.

Fig. 3B - Represents the mean IV curve obtained by measuring the unit currents from original traces from 6 patch clamp experiments with TCE cells ($N = 6$). The conductance (G) and reversal potential (E_R) were obtained by linear regression. The single-channel conductance was 35 ± 1.4 pS for the positive and 17 ± 1 pS for the negative applied voltages. The reversal potential obtained was -0.73 ± 0.8 mV.

Inset 3C - Shows the concentration of Na^+ , K^+ and Cl^- in the pipette and in the bath solution and the respective calculated reversal potentials (E_R).

Figure 4 represents another group of experiments performed with 7 TCE cells in the excised inside-out configuration ($N = 7$). The unit currents (in pA) were measured. Inset 4B shows the concentration of Na^+ , K^+ and Cl^- in the pipette and in the bath solutions and the respective reversal potentials calculated for these experimental conditions. In the resulting IV curve (figure 4A) unit currents (in pA) were plotted against the applied voltages (in mV). This IV relationship presented rectification and the conductances obtained for the positive and negative voltages were 67 ± 1.2 pS and 15 ± 0.6 pS, respectively. The reversal potential obtained was $+1.44 \pm 0.7$ mV. The reversal potential was not statistically different from the one expected for Cl^- in these experimental conditions (0 mV) for an error of the second kind < 0.05 ($t = 2.043$; $p = 0.087$; $f = 6$).

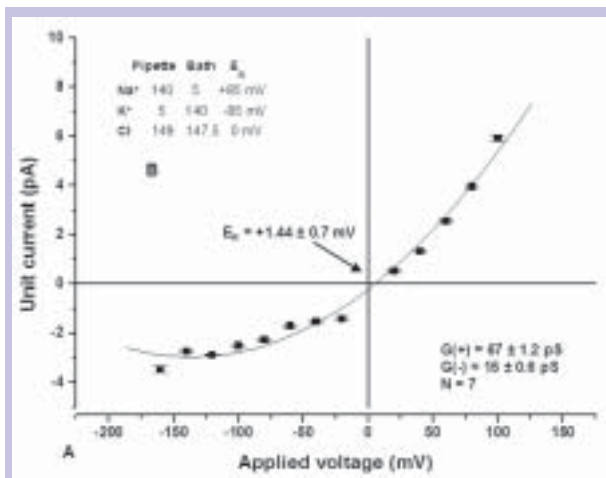


Fig. 4A - Represents an IV curve, where mean unit currents (in pA) obtained from 7 different TCE cells ($N = 7$) were plotted against the applied voltage (in mV). The voltage protocol consisted in 14 steps of 20 mV ranging from -160 mV to +100 mV. The unit currents were measured in original traces obtained in the excised inside-out configuration. Solutions B1 and P1 (see table I) were used in the bath and in the pipette, respectively. The conductance (G) and reversal potential (E_R) were obtained by linear regression. The conductances obtained for the positive and negative voltages were 67 ± 1.2 pS and 15 ± 0.6 pS, respectively. The reversal potential obtained was $+1.44 \pm 0.7$ mV.

Inset 4B - Shows the concentration of Na^+ , K^+ and Cl^- in the pipette and in the bath solution and the respective calculated reversal potentials (E_R).

Excised inside-out unit currents from 7 TCE cells ($N = 7$) in which a sequence of recordings made before and during the addition of 100 mM cAMP and 100 mM IBMX to the bath solution were also analyzed. Figure 5A shows an original trace of current (in pA) versus time (in ms) at the applied voltage of -120 mV, before and 2 minutes after the addition of cAMP and IBMX to the bath solution of one excised inside-out patch. Figure 5B represents the resulting mean IV curve 2 minutes after addition of 100 mM cAMP and 100 mM IBMX to the bath solution, evidencing a linear relationship, a single channel conductance of 14 ± 0.2 pS and a reversal potential of $+0.8 \pm 0.65$ mV. The E_{Cl} calculated for Cl^- under these experimental conditions (see inset 5B) was 0 mV. The reversal potential was not statistically different from the one expected for Cl^- for an error of the second kind < 0.05 ($t = 1.202$; $p = 0.274$; $f = 6$). cAMP and IBMX triggered the appearance of channel activity in otherwise silent membrane patches. Inset 5C shows the concentration of Na^+ , K^+ and Cl^- in the pipette and in the bath solutions and the respective reversal potentials for these experimental conditions.

Figure 6 represents a group of experiments performed with 5 TCE cells in the excised inside-out configuration ($N = 5$). Figure 6A shows an original trace of current (in pA)

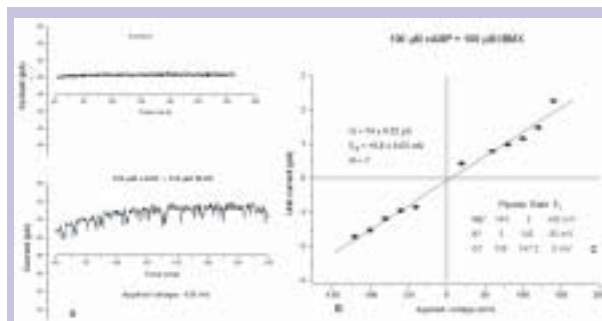


Fig. 5A - Shows an original trace of current (in pA) versus time (in ms) at the applied voltage of -120 mV, before and 2 minutes after the addition of 100 mM cAMP and 100 mM IBMX to the bath solution of one excised inside-out patch.

Fig. 5B - Shows an IV curve, where mean unit currents (in pA) were plotted against the applied voltage (in mV). The voltage protocol consisted in 14 steps of 20 mV ranging from -120 mV to +140 mV. The unit currents were measured in 7 TCE cells ($N = 7$) in the presence of 100 mM cAMP and 100 mM IBMX in the bath solution. They were obtained in the excised inside-out configuration. Solutions B1 and P1 (see table I) were used in the bath and in the pipette, respectively. The conductance (G) and reversal potential (E_R) were obtained by linear regression, evidencing a linear relationship, a single channel conductance of 14 ± 0.2 pS and a reversal potential of $+0.8 \pm 0.65$ mV.

Inset 5C - Shows the concentration of Na^+ , K^+ and Cl^- in the pipette and in the bath solution and the respective calculated reversal potentials (E_R).

versus time (in ms) at different steps of voltage protocol. In the resulting IV curve (figure 6B) mean unit currents (in pA) were plotted against the applied voltages (in mV). This IV relationship presented a linear relationship. The conductance and the reversal potential obtained were 25 ± 7 pS and $+1.8 \pm 1$ mV, respectively. The value calculated for E_{Cl} under these experimental conditions was 0 mV. The

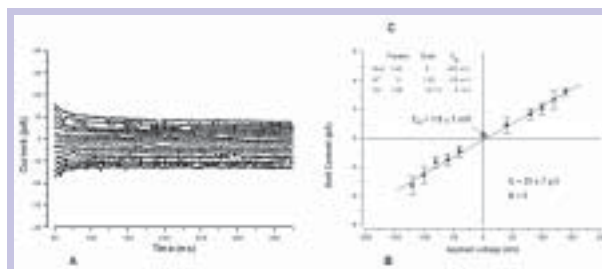


Fig. 6A: Represents original trace of current (in pA) versus time (in ms) obtained in the excised inside-out configuration. The voltage protocol consisted in 14 steps of 20 mV ranging from -120 mV to +140 mV. Solutions B1 and P1 (see table I) were used in the bath and in the pipette, respectively.

Fig. 6B - Reports the resulting mean single channel IV curve obtained from the analysis of original traces with 5 TCE cells ($N = 5$). The conductance (G) and the reversal potential (E_R) were obtained by linear regression. The conductance and the reversal potential obtained were 25 ± 7 pS and $+1.8 \pm 1$ mV, respectively.

Inset 6C - Shows the concentration of Na^+ , K^+ and Cl^- in the pipette and in the bath solution and the respective calculated reversal potentials (E_R) for these experimental conditions.

reversal potential was not statistically different from the one expected for Cl^- for an error of the second kind < 0.05 ($t = 1.56$; $p = 0.193$; $f = 4$). Inset 6C shows the concentration of Na^+ , K^+ and Cl^- in the pipette and in the bath solutions and the respective reversal potentials calculated for these experimental conditions.

DISCUSSION

Complete absence or great reduction of cAMP-stimulated Cl^- conductance at the plasma membrane of epithelial cells is the hallmark of CF, resulting from different mutations in the gene coding for the CFTR protein. To investigate the function of CFTR in biological systems, short-circuit currents in Ussing chambers and patch-clamp techniques are widely used. Most of the studies on CFTR and on its role in airway cell physiology, however, have been conducted in either primary cell cultures or in permanent cell lines, transfected with wild type (wt) or mutant CFTR. On the other hand, CFTR expression has been shown to critically depend on the differentiation and polarization status of epithelia²⁰. In the present work, we have used freshly isolated TCE cells from non-CF individuals obtained by the nasal brushing technique. The yield of nasal cells recovered by this noninvasive technique is good and it has the advantage of avoiding the enzymatic treatment of cells that might alter the membrane structure and permeability. This study was thus, intended at characterizing the Cl^- transport at the sub-apical region of TCE cells (ciliated and non-ciliated) from non-CF individuals, by the patch-clamp technique. We used the cell-attached and the excised inside-out configurations of the patch clamp technique to measure single-channel conductance and reversal potential. The application of these patch clamp configurations to TCE cells freshly isolated has not been described before. Grygorczyk and Bridges in 1992 studied Cl^- conductances in primary cultures of similar nasal cells by the patch-clamp technique, using the whole-cell configuration³². Although using cultured material, those authors demonstrated that human nasal epithelium possesses Cl^- conductances that are regulated by cell swelling and Ca^{2+} and that it represents a useful *in vitro* model for studying ion transport in the airway epithelium. Results obtained by McCann *et al.* in 1989, also in cultivated human nasal cells studied with the whole-cell patch-clamp technique, suggested that the outwardly rectifying Cl^- channel (ORCC) is the predominant Cl^- conductive pathway³³. They described that these Cl^- currents were regulated by the cAMP-dependent protein kinase and it was a cell-swelling stimulated Cl^- current. Kunzelmann *et al.* in 1995 identified Na^+ and Cl^- conductances in epithelial cells from

nasal polyps (both freshly isolated and in primary cultures) using patch-clamp and microelectrode techniques³⁴. With these methods those authors found identical and relatively low membrane voltages of about -36 mV both in normal and in CF cells. A Cl^- conductance could be activated by cAMP in normal but not in CF cells, whereas Ca^{2+} -dependent Cl^- currents activated by ATP and bradykinin were present in both types of cells. The results presented here indicate that at least three different types of Cl^- channels can be identified in fresh non-cultured nasal cells. Firstly, a large conductance (between 35 and 67 pS), voltage-dependent, outward rectifier which were the most frequent channels found, in accordance to what was already described in cultured cells³³. These channels were observed in both cell-attached and excised inside-out configurations. Secondly, a small conductance (around 14 pS), activated by cAMP and IBMX, voltage independent, and with a linear IV relationship. Indeed, results obtained by a large number of groups showed that CFTR Cl^- channels are regulated by cAMP, have a linear IV relationship, are insensitive to 4,4'-diisothiocyanato-stilbene- 2, 2' - disulfonic acid (DIDS) and blocked by 98% *N*-phenylanthranilic acid (DPC), have a single channel conductance of around 8 pS and are more permeable to Cl^- than to I^- ³⁵. A third group of channels was observed in the excised inside-out configuration, with a conductance around 25 pS, voltage independent, and with a linear IV relationship. Cl^- channels play an important role in the physiology and pathophysiology of epithelia but unfortunately their pharmacology is still poor. It is our intention in the future to apply this technique to TCE cells from CF patients in order to assess its potential as a tool for the diagnosis of CF.

REFERENCES

1. ILLEK B, YANKASKAS JR, MACHEN TE: cAMP and genistein stimulate HCO_3^- conductance through CFTR in human airway epithelia. *Am J Physiol* 1997; 272 (4 Pt 1), L752 - L761.
2. HUG MJ, TAMADA T, BRIDGES RJ: CFTR and bicarbonate secretion by epithelial cells. *News Physiol Sci* 2003; 18: 32 - 42.
3. STUTTS MJ, CANESSA CM, OLSEN JC, HAMRICK M, COHN JA, ROSSIER BC, BOUCHER RC: CFTR as a cAMP-dependent regulator of sodium channels. *Science* 1995; 269: 847 - 850.
4. EGAN M, FLOTTE T, AFIONE S, SOLOW R, ZEITLIN PL, CÂRTER BJ, GUGGINO WB: Defective regulation of outwardly rectifying Cl^- channels by protein kinase A corrected by insertion of CFTR. *Nature* 1992; 358: 581 - 584.
5. HRYCIN DH, GUGGINO WB: Cystic fibrosis transmembrane conductance regulator and the outwardly rectifying chloride channel: a relationship between two chloride channels expressed in epithelial cells. *Clin Exp Pharmacol Physiol* 2000; 27: 892 - 895.
6. BRADBURY NA, JILLING T, BERTA G, SORSCHER EJ, BRIDGES RJ, KIRK KL: Regulation of plasma membrane recycling by

- CFTR. *Science* 1992; 256: 530 - 532.
7. PRINCE LS, WORKMAN RBJ, MARCHASE RB: Rapid endocytosis of the cystic fibrosis transmembrane conductance regulator chloride channel. *Proc Natl Acad Sci U.S.A.* 1994; 91: 5192-5196.
 8. BIWERSI J, EMANS N, VERKMAN AS: Cystic fibrosis transmembrane conductance regulator activation stimulates endosome fusion in vivo. *Proc Natl Acad Sci U.S.A.* 1996; 93: 12484 - 12489.
 9. TAKAHASHI A, WATKINS SC, HOWARD M, FRIZZELL RA: CFTR - dependent membrane insertion is linked to stimulation of the CFTR chloride conductance. *Am J Physiol* 1996; 271: C1887 - C1894.
 10. TOUSSON A, FULLER CM, BENOS DJ: Apical recruitment of CFTR in T84 cells is dependent on cAMP and microtubules but not Ca^{2+} or microfilaments. *J Cell Sci* 1996; 109: 1325 - 1334.
 11. WEBER WM, CUPPENS H, CASIMAN JJ, CLAUSS W, VAN DRIESSCHE W: Capacitance measurements reveal different pathways for the activation of CFTR. *Pflügers Arch* 1999; 438: 561 - 569.
 12. CLIFF WH, FRIZZELL RA: Separate Cl^{-} conductances activated by cAMP and Ca^{2+} in Cl^{-} -secreting epithelial cells. *Proc Natl Acad Sci U.S.A.* 1990; 87: 4956 - 4960.
 13. MORRIS AP, CUNNINGHAM AS, TOUSSON A, BENOS DJ, FRIZZELL RA: Polarization-dependent apical membrane CFTR targeting underlies cAMP-stimulated Cl^{-} secretion in epithelial cells. *Am J Physiol* 1994; 266: 254 - 268.
 14. KNOWLES M, GATZY J, BOUCHER R: Increased bioelectric potential difference across respiratory epithelia in cystic fibrosis. *N Engl J Med* 1981; 305: 1489 - 1495.
 15. HAY JG, GEDDES DM: Transepithelial potential difference in cystic fibrosis. *Thorax* 1985; 40: 493 - 496.
 16. ALTON EW, HAY JG, MUNRO C, GEDDES DM: Measurement of nasal potential difference in adult cystic fibrosis, Young's syndrome, and bronchiectasis. *Thorax* 1987; 42: 815 - 817.
 17. HOFFMANN T, BOHMER O, HULS G, TERBRACK HG, BITTNER P, KLINGMULLER V, HEERD E, LINDEMANN H: Conventional and modified nasal potential-difference measurement in cystic fibrosis. *Am J Respir Crit Care Med* 1997; 155: 1908 - 1913.
 18. HO LP, SAMWAYS JM, PORTEOUS DJ, DORIN JR, CAROTHERS A, GREENING AP, INNES JA: Correlation between nasal potential difference measurements, genotype and clinical condition in patients with cystic fibrosis. *Eur Respir Jour* 1997; 10(9): 2018 - 2022.
 19. JACQUOT J, PUCHELLE E, HINNRSKY J, FUCHEY C, BETTINGER C, SPILMONT C, BONNET N, DIETERLE A, DREYER D, PAVIRANI A: Localization of the cystic fibrosis transmembrane conductance regulator in airway secretory glands. *Eur. Respir. J.* 1993; 6: 169 - 176.
 20. BRÉZILLON S, DUPUIT F, HINNRSKY J, MARCH V, KÁLIN N, TÜMMLER B, PUCHELLE E: Decreased expression of the CFTR protein in remodeled human nasal epithelium from non-cystic fibrosis patients. *Lab Invest* 1995; 72:191 - 200.
 21. BECK S, PENQUE D, GARCIA S, GOMES A, FARINHA C, MATA L, GULBENKIAN S, GIL-FERREIRA K, DUARTE A, PACHECO P, BARRETO C, LOPES B, CAVACO J, LAVINHA J, AMARAL MD: Cystic fibrosis patients with the 3272-26A>G mutation have mild disease, leaky alternative mRNA splicing, and CFTR protein at the cell membrane. *Hum Mutat* 1999; 14:133 - 144.
 22. RAMALHO AS, BECK S, MEYER M, PENQUE D, CUTTING GR, AMARAL MD: Five percent of normal cystic fibrosis transmembrane conductance regulator mRNA ameliorates the severity of pulmonary disease in cystic fibrosis. *Am J Resp Cell Mol Biol* 2002; 27(5): 619 - 627.
 23. PENQUE D, MENDES F, BECK S, FARINHA C, PACHECO P, NOGUEIRA P, LAVINHA L, MALH R, AMARAL MD: Cystic fibrosis F508del patients have apically localized CFTR in a reduced number airway cells. *Lab Invest* 2000; 80: 857 - 868.
 24. CARVALHO-OLIVEIRA I, EFTHYMIADOU A, TZETIS M, KANAVAKIS E, MALHO R, AMARAL MD, PENQUE D: Localization of CFTR in airway cells of Cystic Fibrosis patients and controls and cell lines expressing wild-type or F508del-CFTR by a panel of different antibodies. *J Histochem Cytochem* 2004; 52(2), 193 - 203.
 25. DUARTE A, AMARAL M, BARRETO C, PACHECO P, LAVINHA J: Complex cystic fibrosis allele R334W-R1158X results in reduced levels of correctly processed mRNA in a pancreatic sufficient patient. *Human Mutat* 1996; 8: 134 - 139.
 26. DACIE JV, LEWIS SM: *Practical Haematology*. Edinburgh. Churchill Livingstone 1985.
 27. DANIEL C, ERZURUM SC, MCELVANEY NG, CRYSTAL RG: Quantitative assessment of the epithelial and inflammatory cell populations in large airways of normal and individuals with cystic fibrosis. *Am J Respir Crit Care Med* 1996; 153: 362 - 368.
 28. GREGORY RJ, CHENG SH, RICH DP, MARSHALL J, PAUL S, HEHIR K, OSTEDGAARD L, KLINGER KW, WELSH MJ, SMITH AE: Expression and characterization of the cystic fibrosis transmembrane conductance regulator. *Nature* 1990; 347: 382 - 386.
 29. HAMILL OP, MARTY A, NEHER E, SACKMANN B, SIGWORTH FJ: Improved patch - clamp techniques for high-resolution current recording from cells and cell - free membrane patches. *Pflügers Arch* 1981; 391: 85 - 100.
 30. HALD A: *Statistical Theory with Engineering Applications*, pp. 391-394. John Wiley, New York, 1952.
 31. FERREIRA KTG, FERNANDES PL, FERREIRA HG: Ion transport across the epithelium of the rabbit caecum. *Biochimica et Biophysica Acta* 1992; 1175: 27 - 36.
 32. GRYGORCZYK R, BRIDGES MA: Whole-cell chloride conductances in cultured brushed human nasal epithelial cells. *Can J Physiol Pharmacol* 1992; 70(8): 1134 - 1141.
 33. MCCANN JD, LI M, WELSH MJ: Identification and regulation of whole-cell chloride currents in airway epithelium. *J Gen Physiol* 1989; 94(6): 1015 - 1036.
 34. KUNZELMANN K, KATHÖFER S, GREGER R: Na^{+} and Cl^{-} conductances in airway epithelial cells: Increased Na^{+} conductance in cystic fibrosis. *Pflügers Arch* 1995; 431: 1 - 9.
 35. SCHWIEBERT EM, FLOTTE T, CUTTING GR, GUGGINO WB: Both CFTR and outwardly rectifying chloride channels contribute to cAMP- stimulated whole cell chloride currents. *Am J Physiol* 1994; 266: C1464 - 1477.